Tunability of absorption threshold frequencies and Stark shift in spherical quantum layer

Eduard M. Kazaryan[a], Albert A. Kirakosyan[b], Vram N. Mughnetsyan[b], Hayk A. Sarkisyan[a,b]
[a]Russian-Armenian (Slavonic) University, Yerevan, Armenia
[b]Yerevan State University, Yerevan, Armenia

ABSTRACT

In the present work the interband optical absorption in the ensemble of spherical quantum layers with weak quantum interaction is investigated. The distribution of layers by their inner radii is taken into account. The effect of weak electric field on the energy levels coupling and absorption character is investigated as well. It is shown that the energy spectrum 1s1p1d2s1f2p… for spherical quantum dot turns to the spectrum 1s1p1d1f2s2p… for spherical quantum layer with enough large value of inner radius. It is also shown that in spherical quantum layer, where the coupling between neighboring states is not negligible, there is no square low dependence of Stark shift on electric field strength in contrast to the rotator model.

Keywords: spherical quantum layer, absorption coefficient, Stark shift

1. INTRODUCTION

The experimental realization of layered and ring-like semiconductor nanostructures makes it possible to consider a range of solid state quantum mechanical problems in which electronic, optical, and other characteristics of such systems are observed[1-5]. The non-trivial geometry of layered nanostructures gives an opportunity of energy spectrum flexible manipulation by means of size and geometrical shape variation. The theoretical results obtained for layered nanostructures have a general character and can be used for description of nanostructures with other geometries which are the limiting cases of layered nanostructures. Indeed, if one consider a layered quantum dot with inner R_1 and outer R_2 radii and with height L, then as limiting cases one can get from this structure 1. a cylindrical quantum dot ($R_1 \to 0, R_2 = const, L = const$), 2. a quantum well-wire with the cylindrical cross section $R_1 \to 0, R_2 = const, L \to \infty$, and 3. a quantum well ($R_1 \to 0, R_2 \to \infty, L = const$). It is clear that the strong dependence of the charge carrier energy spectrum on geometrical parameters of layered nanostructures makes an opportunity to consider these structures as a base element for new generation devices. Along with practical importance, structures with the layered geometry allow to realize experimental examination of fundamental principles of modern physics. In particular, the experimental realization of quantum rings made possible the examination of Aharonov-Bohm effect for confined states and the Aharonov-Bohm oscillations for the ground state of electron in the presence of axially directed magnetic field. Spherical quantum layers[6] (SQL) are structures that are interesting to investigate because they demonstrate effects that are inherent both to quantum wells and to curved (spherical) surfaces. In this connection SQL has a number of common properties with fullerenes. Electronic, optical and other properties of SQLs have been widely investigated by a variety of authors[7-10].

Thus SQLs may have a wide application in nanoelectronics as an active medium for the optoelectronic devices of new generation and the deep understanding of optoelectronic processes in these structures is of great interest. One of crucial problems is the investigation of the tunability of optical absorption threshold by changing of the geometrical parameters of SQL in the presence or the absence of external fields. In the present work the interband optical absorption in the ensemble of SQL with weak quantum interaction is investigated. The effect of weak electric field on the absorption character is considered as well.

Photonics and Micro- and Nano-structured Materials 2011, edited by Rafael Kh. Drampyan,
Proc. of SPIE Vol. 8414, 84140B · © 2012 SPIE · CCC code: 0277-786X/12/$18 · doi: 10.1117/12.923126

2. ENERGY SPECTRUM

The Schrodinger equation for the SQL in the effective mass μ approximation is

$$\left\{-\frac{\hbar^2}{2\mu}\nabla^2 + V_{conf}(r)\right\}\psi(\vec{r}) = E\psi(\vec{r})\,. \tag{1}$$

The confining potential in (1) is given by the expression:

$$V_{conf}(r) = \begin{cases} 0, & |r - R_{eff}| \le d/2, \\ \infty, & |r - R_{eff}| > d/2, \end{cases} \tag{2}$$

where R_1 and R_2 are the inner and outer radii respectively, $R_{eff} = (R_1 + R_2)/2$ is the effective radius and $d = R_2 - R_1$ is the width of SQL.

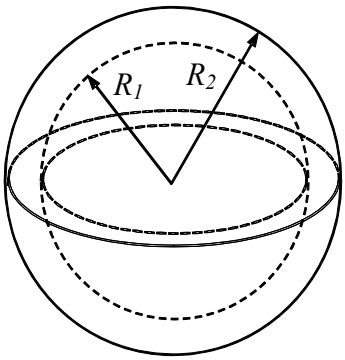

Figure1. The schematic form of SQL.

In Fig.1 the schematic view of SQL is presented. It is obvious that the electron is confined between the inner and outer infinitely high barriers.

Since the confining potential has spherical symmetry the electron's wave function in spherical coordinates can be presented as:

$$\psi_{n_r,l,m}(r,\theta,\varphi) = f_{n_r,l}(r)Y_{l,m}(\theta,\varphi)\,, \tag{3}$$

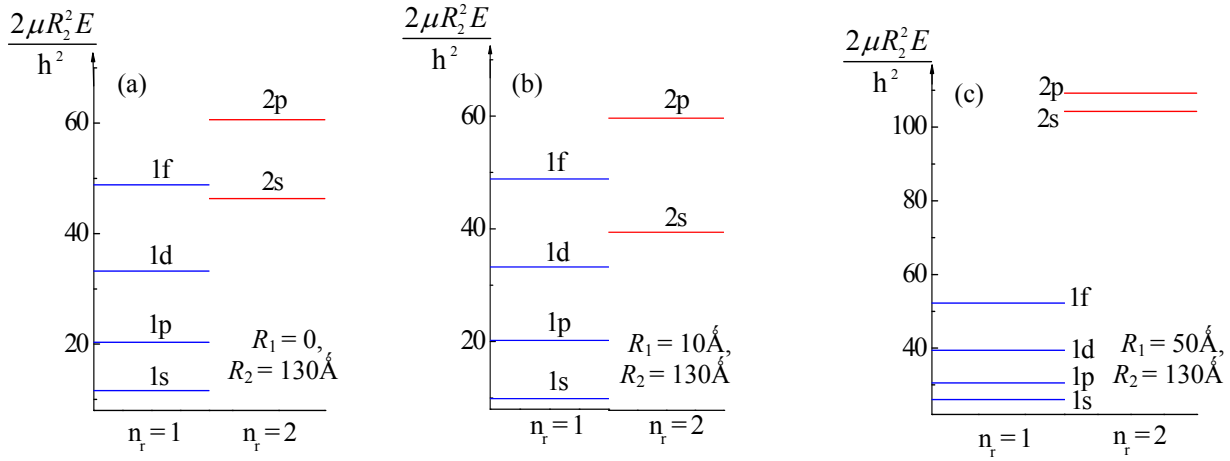

Figure 2. The energy diagram for QD (a), and SQL with different inner radii ((b) and (c)).

where $Y_{l,m}(\theta,\varphi)$ are the spherical harmonics. The radial part of the wave function satisfying equation (1) with confining potential (2) is[11]:

$$f_{n_r,l}(r)=\frac{1}{\sqrt{r}}(C_1 J_{l+1/2}(k_{n_r}r)+C_2 J_{-(l+1/2)}(k_{n_r}r)), \tag{4}$$

where $k_{n_r}=\sqrt{2\mu E/\hbar^2}$, $J_\nu(k_{n_r}r)$ is the Bessel function of the first kind, C_1 and C_2 are constants. The energy spectrum of considered system can be obtained from the boundary conditions $f_{n_r,l}(R_{1(2)})=0$, which leads to the equation

$$\det \mathrm{J}=\begin{vmatrix} J_{l+1/2}(kR_1) & J_{-(l+1/2)}(kR_1) \\ J_{l+1/2}(kR_2) & J_{-(l+1/2)}(kR_2) \end{vmatrix}=0. \tag{5}$$

In Fig.2 the energy diagrams of spherical quantum dot (SQD) (Fig.2a) and SQL with the inner radii 10Å (Fig.2b) and 50Å (Fig.2c) are presented. It is clear that for enough small values of the SQL inner radius the sequence of the energy levels is similar to the one for SQD (1s1p1d2s1f2d…) of the same radius as the outer radius of SQL (Fig.2a and b). For larger values of R_1 (Fig.2c) one can observe another sequence of energy levels (1s1p1d1f2s2d…). The influence of increasing of the radial quantum number on the energy levels is as greater as larger the inner radius is.

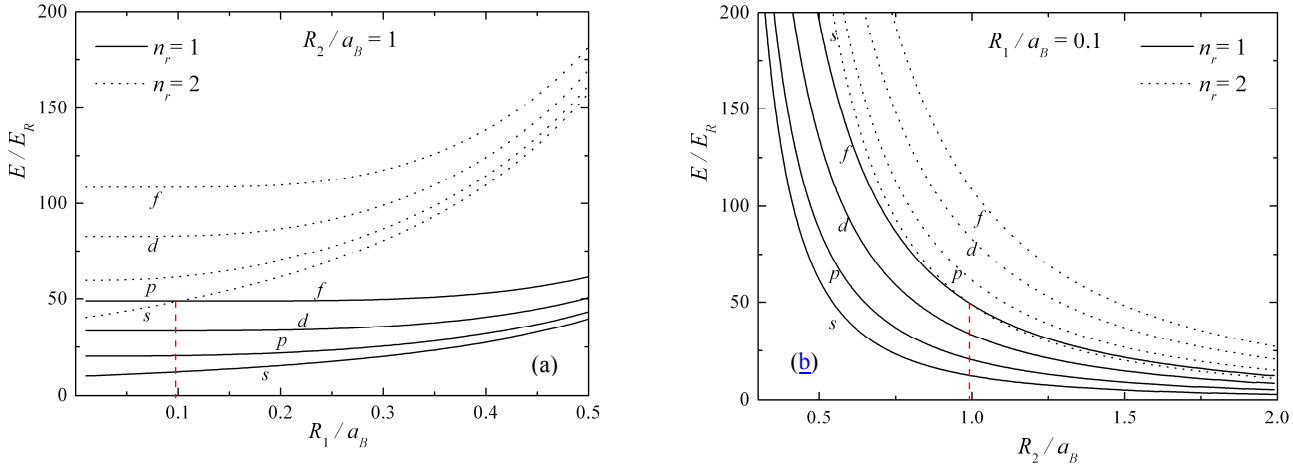

Figure 3. Dependences of the electron energy on inner (a) and outer (b) radii of SQL.

The dependences of electron dimensionless energy values (E_R is the Rydberg energy for the considered structure) on inner and outer radii of SQL are presented on Fig.3a and Fig.3b respectively. In Fig.3a one can observe an obvious increase of electron energy values with the increase of the SQL inner radius because of the enhancement of the size quantization (the outer radius is fixed). Note that the values of electron energy for the case $R_1=0$ coincide with the electron energy levels in SQD with the radius equal to the outer radius of SQL. The increase of the energies corresponding to the radial quantum number $n_r=2$ occurs more rapidly that in the case of $n_r=1$ and the curves corresponding to 1f and 2s states are intersected approximately at $R_2=0.1a_B$. This is the point where the transformation of energy levels sequence occurs. In Fig.3b there is an opposite situation comparing with the Fig.3a. Namely, the size quantization becomes weaker with the increase of the outer radius of SQL with the fixed inner radius, resulting to the decrease in the energy of quantization. For the given value of outer radius $R_2 \approx 1a_B$ the transformation $1s1p1d1f2s2p \rightarrow 1s1p1d2s1f2p$ occurs.

3. INTERBAND ABSORPTION

Let us consider the interband absorption in SQL structure. The absorption coefficient is defined by well known expression[12]:

$$K^{h\to e}(\omega,R_1,R_2)=\frac{A}{V}\sum_{\nu,\nu'}\left|\int\Psi^e_\nu\Psi^h_{\nu'}dV\right|^2\delta\left(\hbar\omega-E_g-E^e_\nu-E^h_{\nu'}\right), \tag{6}$$

where

$$A=\frac{\pi e^2}{m_0\varepsilon_0 cn\omega}\frac{P^2_{cv}}{3},$$

$P_{cv}=-i\hbar\int_{\Omega_0}U^*_c\vec{\nabla}U_v d\Omega$ is the dipole momentum matrix element for the Bloch functions, n is the refractive index, m_0 is the free electron mass, ε_0 is the dielectric permittivity of vacuum. Also E^e_ν and $E^h_{\nu'}$ are the electron and hole energies which are considered from the conduction and the valence band edges respectively, E_g is the band gap width. Taking into account the expression (3) for the envelope functions of electron and heavy hole we obtain the following selection rules from (6):

$$n_r=n'_r, \qquad l=l', \qquad m=m' \tag{7}$$

and arrive to the following expression for absorption coefficient:

$$K^{h\to e}(\omega,R_1,R_2)=\frac{A}{V}\sum_{l,n_r}(2l+1)\delta\left(\hbar\omega-E_g-E^e_{n_r,l}-E^h_{n_r,l}\right), \tag{8}$$

where V is the volume of the sample.

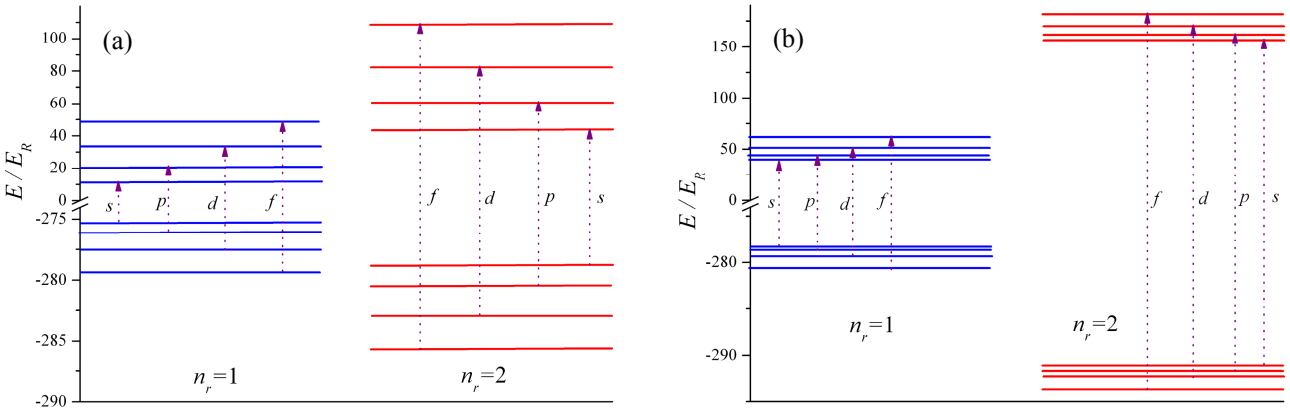

Figure 4. Interband transition diagrams in SQL with the parameter values *a*: R_1 = 5Å, R_2 = 100Å, and *b*: R_1 = 50Å, R_2 = 100Å.

The interband absorption diagrams in SQL with the different values of inner radius are presented in Fig.4. Firstly, it is obvious that the only transitions indicated by arrows are allowed due to the selection rules (7). Secondly, as it was already mentioned, the sequence of the energy levels depends on the value of SQL inner radius. The change of the energy levels sequence leads to the change of the sequence of absorption thresholds and in contrast to the case of SQD in SQL with enough small width the transitions between 1f states occur at smaller values of incident photon energy, than the transitions between 2s states. Finally it is clear from the Fig.4 that the difference between the absorption thresholds which correspond to different values of n_r are significantly larger for the larger value of the inner radius.

Assuming that there is a Gaussian distribution of inner radii in the ensemble of SQL

$$P(\bar{R}_1, R_1) = \frac{1}{\sqrt{2\pi}\sigma_{R_1}} \exp\left[-\frac{(R_1 - \bar{R}_1)^2}{2\sigma_{R_1}^2} \right], \tag{9}$$

with the characteristic width σ_{R_1} one can calculate the absorption coefficient of this system as follows:

$$K(\omega, \bar{R}_1, R_2) = \int_0^{R_2} K^{h\to e}(\omega, R_1, R_2) P(\bar{R}_1, R_1) dR_1 \,. \tag{10}$$

Substituting (8) and (9) in (10) we derive the following expression:

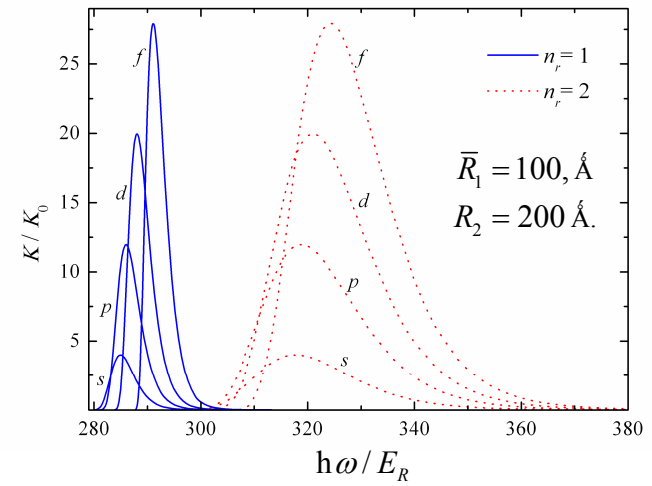

Figure 5. Dependence of interband absorption coefficient on dimensionless energy of incident photon.

$$\frac{K(\omega, \bar{R}_1, R_2)}{K_0} = \frac{1}{\sqrt{2\pi}\sigma_{R_1}} \sum_{n_r, l} (2l+1) \exp\left[-\frac{(r_1(\omega) - \bar{R}_1)^2}{2\sigma_{R_1}^2} \right], \tag{11}$$

where $K_0 = A/V$ and the function $r_1(\omega)$ is obtained from the following equation,

$$E^e_{n_r, l}(r_1) + E^h_{n_r, l}(r_1) + E_g - \hbar\omega = 0 \,. \tag{12}$$

In Fig.5 we have presented the dependences of the interband absorption coefficient of the ensemble of SQL on incident photon energy (σ_{R_1} is taken to be 10Å). First of all we see that the curves have continuous behavior due to the distribution of SQLs by their inner radii. The absorption spectrum which corresponds to $n_r = 2$ is shifted to the right due to the larger value of absorption threshold and is wider due to the stronger effect of the variations of the SQL inner radius on the energies corresponding to $n_r = 2$. It is noticeable that the peaks of the absorption spectrum are higher for the larger values of the azimuthal quantum number *l*. This fact is explained by the difference of the angular distribution of electrons probability density in SQL. Namely for *l* = 0 (*s* states) the wave function has spherical symmetry, as a result of which the energy levels are more sensitive in respect to the changes of SQL inner radius comparing with the case of *l* = 1 (*p* states). The sensitiveness of energy levels in respect to SQL inner radius changes leads to the larger distribution of absorption coefficient by the photon energy and to the smaller value of the spectrum peaks. The difference of the angular distribution of wave function from the spherical symmetric one is as more as larger the value of *l* as a result of which we have the sequence of the curves as mentioned in the figure.

4. STARK SHIFT

In this section we consider the influence of external uniform electric field on the electron energy spectrum (Stark shift) in SQL. The Stark shift of energy levels is well known for spherical rotator which is the limiting case of SQL when $d = R_2 - R_1 \to 0$. In this model the energy levels are defined as follows[13]:

$$E_{rot} = \hbar^2 l(l+1)/2\mu R_{eff}^2 . \tag{13}$$

Considering the case of uniform electric field, the electric potential term will have the following form:

$$\hat{V}(\theta,\varphi) = -p\left(F_x \sin\theta\cos\varphi + F_y \sin\theta\sin\varphi + F_z \cos\varphi\right), \tag{14}$$

where p is dipole momentum of electron, $\vec{F}$ is electric field strength. Based on perturbation theory it is possible to show that the influence of electric field is defined by the second order perturbation integral

$$\left\langle l', m' \middle| \hat{V} \middle| l, m \right\rangle = \int\int Y^*_{l',m'} \hat{V}(\theta,\varphi) Y_{l',m'} \sin\theta d\theta d\varphi . \tag{15}$$

After some transformations we find that the Stark shift is proportional to the square of electric field strength

$$\Delta E_{l,m} = \frac{p^2 J}{2\hbar^2} F^2 \left(2\cos^2\theta - \sin^2\theta\right) \frac{l(l+1) - 3m^2}{(2l+3)(2l-1)l(l+1)} \tag{16}$$

The situation is different, in some sense, in the case of SQL, when the coupling between neighboring states is not negligible. Without violating the generality one can assume that the vector of electric field strength $\vec{F}$ is directed along the *z* axis. For simplification of calculations we assume that there is only coupling between the states 1*s* and 1*p*, which is reasonable for SQL with enough small ratio of d / R_{eff}. The Schrödinger equation for considered system is

$$(\hat{H}_0 + \hat{H}')\Psi(r,\theta,\varphi) = E\Psi(r,\theta,\varphi) , \tag{17}$$

where $\hat{H}_0$ is the Hamiltonian in the absence of electric field, $\hat{H}'(F,r,\theta) = -eFr\cos\theta$ is the perturbation operator. The wave function is taken to be a superposition of the wave functions of 1s and 1p states[14]:

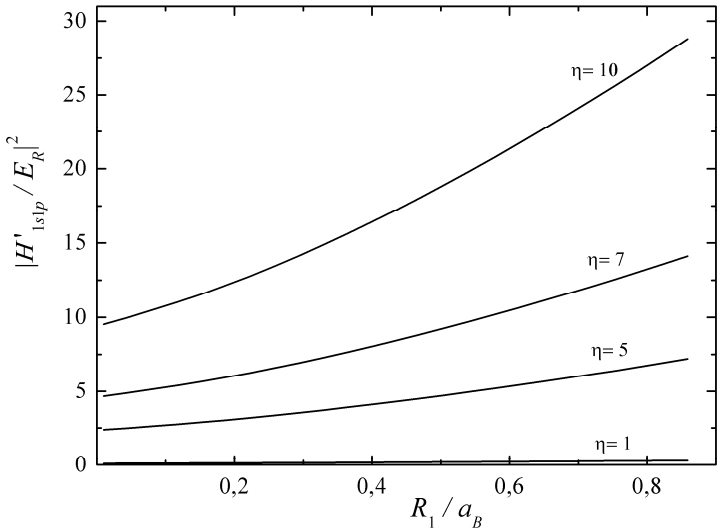

Figure 6. Dependence of overlap integral on inner radius

$$\Psi(r,\theta,\varphi) = C_1\psi_{1s}(r,\theta,\varphi) + C_2\psi_{1p}(r,\theta,\varphi)\,. \tag{18}$$

Substituting (18) into (17) we find the following expression for the energy levels of the first two states:

$$\mathbf{E}_{1s(1p)} = \frac{E_{1s}+E_{1p}}{2} - (+)\frac{1}{2}\sqrt{(E_{1s}-E_{1p})^2 + 4\,|\,H'_{1s1p}\,|^2}\,, \tag{19}$$

where

$$|\,H'_{1s1p}\,|^2 = \frac{(Fe)^2}{3}\left(\int_{R_1}^{R_2} f_{1s}(r)f_{1p}(r)r^3dr\right)^2 \tag{20}$$

is the square of the matrix element between two states, $E_{1s(1p)}$ is the energy of the first (second) state in the absence of electric field. Note that this matrix element provides the second correction of the energy value, whereas the first one which is given by the average value of the perturbation operator in each state is zero due to the wave function symmetry with respect to $z = 0$ plane. The dependence of the dimensionless matrix element on inner radius of SQL for different radii of dimensionless electric field strength ($\eta = eFa_B / E_R$) is presented in Fig.6. The obvious increase of the matrix element is due to the increase of the overlap of the wave functions which correspond to the 1*s* and 1*p* states. In addition, the increase of the matrix element is as quickly as greater the value of electric field strength is, because of the increase of the localization degrees in both states.

The Stark shift of the energy levels in this case is defined by the following expression:

$$\Delta E_{1s(1p)} = \mathbf{E}_{1s(1p)} - E_{1s(1p)}\,. \tag{21}$$

The dependences of 1s and 1p states' Stark shift on the inner radius of SQL and dimensionless electric field strength are presented in Fig.7. The obvious increase of $|\,\Delta E\,|$ with the increase of R_1 in Fig.7a is caused by the increase of the overlap integral in (20) due to the increasing of quantization degree in SQL. On the other hand the Stark shifts of 1s and 1p states have opposite signs and the same absolute values ($\Delta E_{1s} = |\,\Delta E_{1s}\,| = -\Delta E_{1p}$) as follows from (19). This kind of behavior of the first two states is well understood for quantum wells and is because of linear dependence of the potential on *z* coordinate. It is also clear from the Fig 7a that the increase of electric field strength leads to the stronger dependence of ΔE on R_1 due to the stronger effect of the coupling between two states on energy levels. Observing Fig.7b, one can see that the increase of η also results to the increase of ΔE and in the case of $\eta = 0$ there is no shift in energy levels. The effect of electric field on energy levels is as stronger as larger the value of the inner radius is. This effect is directly caused by the coupling of the states and can not be observed in the framework of remote levels approach.

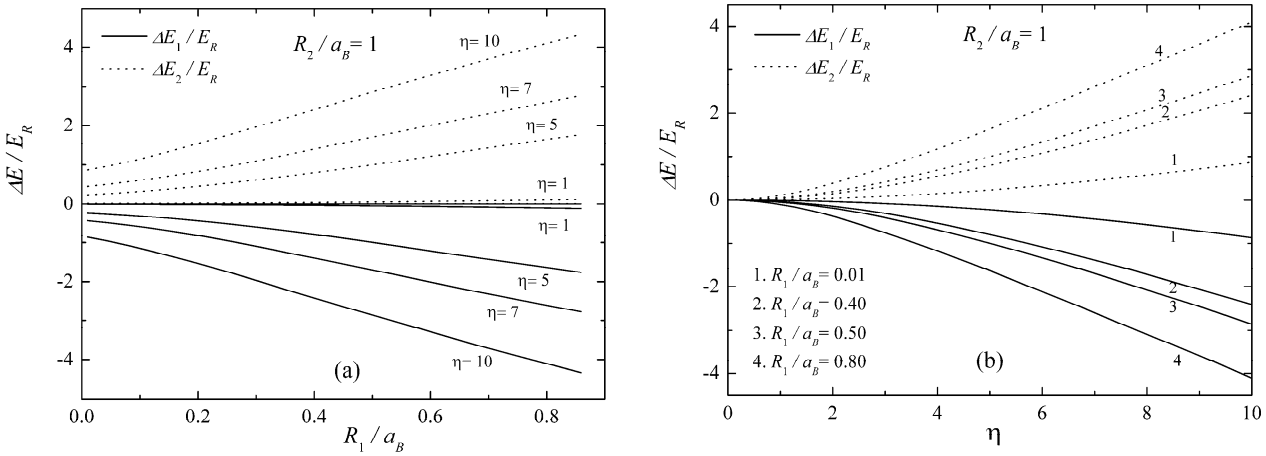

Figure 7. Dependences of the Stark shift of the 1s and 1p states energies on the SQL inner radius (a) and dimensionless electric field strength (b).

Summarizing we can conclude that the strong quantization of electron motion in SQL by inner and outer radii leads to the change in the energy spectrum sequence comparing with the case of SQD. Namely the spectrum 1s1p1d2s1f2p… for SQD turns to the spectrum 1s1p1d1f2s 2p… for SQL with enough large value of inner radius. In contrast to SQD in SQL with enough small width transitions between 1f states occur at smaller values of incident photon energy, then transitions between 2s states. In SQL, where the coupling between neighboring levels is not negligible, one can find more complicated dependence of Stark shifts on electric field strength comparing with the case of rotator model, where the square dependence takes place.

ACKNOWLEDGMENT

The research of one of the authors (Dr. V.N. Mughnetsyan) was supported by Armenian State Committee of Science (Project No. 11B-1c039).

REFERENCES

[1] Lorke, Axel; Johannes Luyken, R.; Govorov, Alexander O.; Kotthaus, Jörg P.; Garcia, J. M.; Petroff, P. M., "Spectroscopy of Nanoscopic Semiconductor Rings", Physical Review Letters, 84, 2223-2226 (2000).
[2] Chakraborty, T., "Nanoscopic Quantum Rings: A New Perspective" Advances in Solid State Physics, 43, 79-94 (2003).
[3] Chen, Hong-Yi; Pietiläinen, Pekka; Chakraborty, Tapash, "Some unique magnetic properties of nanoscale quantum rings subjected to a Rashba spin-orbit interaction", Physical Review B, 78, 073407 (2008).
[4] Kálmán, Orsolya; Földi, Péter; Benedict, Mihály G.; Peeters, F. M., "Magnetoconductance of rectangular arrays of quantum rings", Physical Review B, 78, 125306 (2008).
[5] Čukarić, N.; Tadić, M.; Peeters, F. M., "Electron and hole states in a quantum ring grown by droplet epitaxy: Influence of the layer inside the ring opening", Superlattices and Microstructures, 48, 491-501 (2010).
[6] Kim S., Park J., Kim T., Jang E., Jun S., Jang H., Kim B., Kim S.-W, "Reverse type-I ZnSe/InP/ZnS core/shell/shell Nanocrystals: Cadmium-Free Quantum Dots for Visible Luminescence", Small, 7, 70-73 (2011).
[7] Harutyunyan, V. A.; Aramyan, K. S.; Petrosyan, H. Sh.; Demirjian, G. H., "Optical transitions in spherical quantized layer under the presence of radial electrical field", Physica E, 24, 173-177 (2004).
[8] Boz, F. K.; Aktas, S.; Bilekkaya, A.; Okan, S. E., "The multilayered spherical quantum dot under a magnetic field", Applied Surface Science, 256, 3832-3836 (2010).
[9] Zoheir, M.; Manaselyan, A. Kh.; Sarkisyan, H. A., "Electronic states and the Stark shift in narrow band InSb quantum spherical layer", Physica E, 40, 2945-2949 (2008).
[10] Aghekyan, N. G.; Kazaryan, E. M.; Kostanyan, A. A.; Sarkisyan, H. A., "Two electronic states in spherical quantum nanolayer", Proceedings of the SPIE, 7998, 79981C-79981C-9 (2010).
[11] Aghekyan, N. G.; Kazaryan, E. M.; Kostanyan, A. A.; Sarkisyan, H. A., "Two electronic states and state exchange time control in spherical nanolayer", Superlattices and Microstructures (2011), doi:10.1016/j.spmi.2011.06.001.
[12] Efros Al., Efros A., "Interband absorption of light in a semiconductor sphere". Soviet Physics Semiconductors, 16, 772-775 (1982).
[13] S. Flugge., [Practical Quantum Mechanics Part 1], Springer, Germany, 1971.
[14] Migdal A., Kraynov V., [Approximate methods of quantum mechanics], Moscow, Nauka Publ. (1966).